ELSEVIER

Earth and Planetary Science Letters 167 (1999) 297–310

EPSL

Hotspot–ridge interaction along the Southeast Indian Ridge near Amsterdam and St. Paul islands: helium isotope evidence

D.W. Graham [a,*], K.T.M. Johnson [b], L. Douglas Priebe [a], J.E. Lupton [c]

[a] *College of Oceanic and Atmospheric Sciences, Oregon State University, Corvallis, OR 97331, USA*
[b] *Bishop Museum, Honolulu, HI 96817, USA*
[c] *NOAA, Pacific Marine Environmental Laboratory, Hatfield Marine Science Center, Newport, OR 97365, USA*

Received 4 June 1998; revised version received 26 January 1999; accepted 29 January 1999

Abstract

We report new helium isotope analyses for basaltic glasses recovered along the Southeast Indian Ridge (SEIR) between longitudes 77ºE and 88ºE. In this region, the SEIR shoals to a depth less than 1800 m as it crosses the Amsterdam–St. Paul (ASP) plateau. Atop the plateau, where the average sample spacing is ~10 km, $^3He/^4He$ ratios range between 9.3 and 13.4 R_A (R_A = atmospheric ratio) with significant variability over short distances. Away from the plateau, ridge segments show a more restricted $^3He/^4He$ range, between 7 and 9 R_A. Elevated $^3He/^4He$ ratios on the plateau are evidence for a deep mantle plume component that has been injected into the sub-ridge mantle beneath the region. Ridge segments southeast of the plateau show lower $^3He/^4He$ (7.6–8.3 R_A) than segments to the northwest (8.3–9.0 R_A), suggesting either a systematically varying 'background contamination' of the MORB asthenosphere in the region, or localized input of a 'low $^3He/^4He$' component along the southeastern ridge segments, possibly derived from the distant Kerguelen hotspot. A double peak structure exists in the regional $^3He/^4He$ spatial distribution, because there is also a strong plume-derived He isotope signal which is offset from the shallowest, thickest section of the ridge. High $^3He/^4He$ ratios (up to 14.1 R_A) are present all along the ridge segment immediately to the northwest of the ASP plateau (segment H), where anomalies in K/Ti ratio are also observed. The high $^3He/^4He$ ratios persist to the northern end of segment H, beyond which they abruptly drop to MORB background levels, which apparently persist all the way to the Rodrigues Triple Junction. This pattern suggests that the high-$^3He/^4He$ ASP plume supplies a shallow north-northeastward mantle flow toward adjacent portions of the SEIR. There is a systematic difference in $^3He/^4He$–K/Ti behavior between axial lavas from the ASP plateau and those from segment H, suggesting a higher He/Ti elemental abundance ratio in the plume source material beneath segment H compared to that beneath the ridge axis on the ASP plateau. These observations are consistent with a model in which plume material supplied to segment H is derived from the outer portions of the ASP plume, where removal of He (relative to Ti) has been less efficient than within the core of the plume located beneath the Amsterdam and St. Paul islands. These outer portions of the plume have lower temperatures and have undergone less partial melting, leading to a higher relative He/Ti ratio compared to the inner portions of the plume that feed portions of the sub-ridge mantle beneath the ASP plateau.

Keywords: helium; isotopes; mantle plumes; Southeast Indian Ridge; mid-ocean ridge basalts

* Corresponding author. Tel.: +1-541-737-4140; Fax: +1-541-737-2064; E-mail: dgraham@oce.orst.edu

0012-821X/99/$ – see front matter
PII: S0012-821X(99)00030-8

1. Introduction

The morphology and composition of a significant fraction of the global mid-ocean ridge system is influenced by the input of heat and mass from nearby mantle plumes. Geochemical patterns related to this influence have been defined at the regional scale (~50 to 100 km) for many hotspot source–spreading ridge systems (e.g., [1–6]), but finer-scale patterns (~10 to 30 km) have not been studied. An understanding of the isotopic and chemical variations at this scale is needed to test current hotspot–ridge interaction models that incorporate parameters such as plume flux and spreading rate [7–11], the possible role of transform faults and fracture zones as barriers to flow [10], and the slope of the rheological boundary at the base of the lithosphere [6,8].

Helium isotope variations in mid-ocean ridge basalts (MORB) are sensitive to the flow and chemical interaction between mantle plumes and nearby ocean ridge spreading centers. Systematic He isotope studies in MORB have been carried out in the North Atlantic [12,13], South Atlantic [14,15] and Pacific Oceans [5,16]. In a global comparison of Sr, Nd and Pb isotope characteristics, Indian Ocean MORB are distinct compared to MORB from the Atlantic and Pacific [17,18], but only reconnaissance studies of helium isotope variations along the Central and Southwest Indian Ridges have been carried out [19]. The Southeast Indian Ridge (SEIR) stretches nearly 6000 km from the Rodrigues Triple Junction to the Australian–Antarctic Discordance. It is a primary locus for basaltic magmatism carrying the Indian Ocean isotope signature, distinguished by its relatively high $^{87}Sr/^{86}Sr$, $^{207}Pb/^{206}Pb$ and $^{208}Pb/^{206}Pb$ ratios [20–23]. It is also the spreading center nearest the Kerguelen–Heard hotspot (located 1000–1200 km to the southwest), a large mantle plume responsible for the creation of the Kerguelen plateau and the Ninety-East Ridge [24]. Schilling [25] assigned Kerguelen the largest volumetric flow of all near-ridge hotspots, and Storey et al. [26] suggested that its dispersion into the upper mantle during opening of the Indian Ocean may have been responsible for the distinctive isotope characteristics of Indian Ocean mantle. The SEIR also passes very close (50 to 80 km) to the Amsterdam and St. Paul islands, as it crosses an approximately 200 × 100 km wide oceanic plateau situated between 78° and 78.5°E longitude. The Amsterdam–St. Paul (ASP) and Kerguelen hotspots have different Sr–Nd–Pb isotope signatures; consequently, the extent of each hotspot's influence could, in principle, be mapped by analyzing basalts erupted at and near the spreading ridge axis. This, in turn, could clarify the nature of mantle flow beneath the SEIR. In the present study we report helium isotope data for basalts from the ASP plateau and nearby SEIR, and discuss the implications for interaction between the ridge and the mantle hotspots of Amsterdam–St. Paul and Kerguelen.

2. Background

The Kerguelen hotspot, located ~1000 km southwest of the ASP plateau (Fig. 1), began forming during the mid-Cretaceous soon after the separation of India from eastern Gondwana [27]. Seafloor spreading began along the SEIR during the Eocene, and caused the Kerguelen plateau and Broken Ridge to separate at the site of the hotspot [28,29]. Since then the SEIR has been migrating to the northeast away from the Kerguelen hotspot. The ASP hotspot was originally located beneath the Australian plate, and its track may have been nearly coincident with that of the Kerguelen hotspot before about 18 Ma [29,30]. After that time the ASP hotspot track appears to be marked by rough gravity anomalies (seamounts) that can be seen in the satellite map of Sandwell and Smith [31] to prominently stretch from the Ninety-East Ridge to the northern edge of the ASP plateau. The migrating SEIR passed over the ASP hotspot within the last few million years. Currently the ASP hotspot lies 50 to 100 km southwest of the SEIR, the exact distance depending on the choice of Amsterdam Island or St. Paul Island as the current hotspot location. Now that the ASP hotspot lies beneath the nearly stationary Antarctic plate, island volcanic edifices are being formed on 3 to 5 million year old seafloor, suggesting an ongoing buildup of the ASP plateau.

There is a pronounced, ~500-km-long, U-shaped deviation of the SEIR in the vicinity of the ASP plateau (Fig. 1). Southeast of the plateau there have been minor ridge jumps that transferred material to the Australian plate, but overall the shape of the ridge

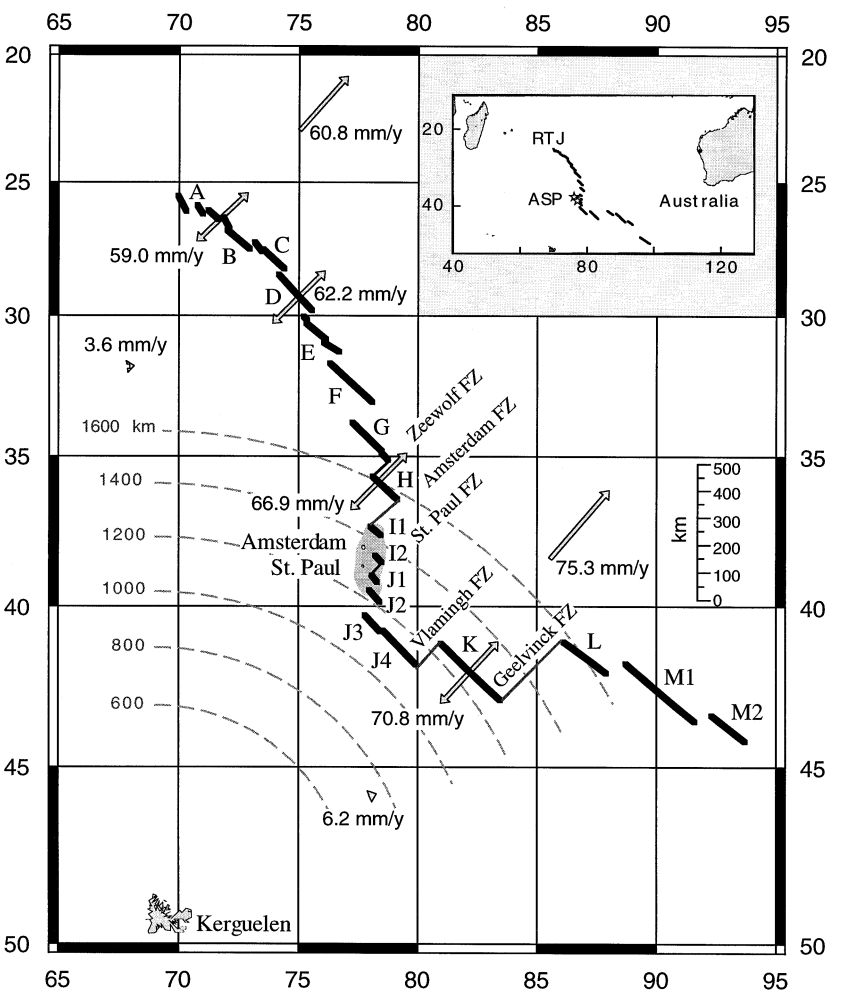

Fig. 1. Segmentation of the Southeast Indian Ridge between the Rodrigues Triple Junction (RTJ) and 92ºE, following the segment designations of Royer and Schlich [33]. The shaded region delineates the 2000 m isobath that encompasses the ASP plateau. Arrows centered on the ridge axis indicate full spreading rate, and away from the ridge axis they indicate absolute plate motion vectors [69]. Radial distance from Kerguelen is indicated by the concentric lines. Inset shows the regional setting for this part of the SEIR.

probably still reflects the original shape at the time of the break-up between Kerguelen plateau and Broken Ridge [28]. A direct influence on crustal accretion along the SEIR by the distant Kerguelen hotspot may also be indicated by the gravity lineations and seamounts that can be seen to trend into the ridge segments located in the southeast portions of our study area [32]. The SEIR between 88ºE and 77ºE is characterized by intermediate spreading rates (60–77 mm/y) along eleven different ridge segments. Following the segment designations of Royer and Schlich [33], full spreading rates are between 60 and 68 mm/y along segments F, G, H and J (Fig. 1), but these increase to the southeast along segments K and L. Four of the ridge segments (I1, I2, J1 and J2) cross the ASP plateau as en-echelon neovolcanic zones having significant overlap. The eleven ridge segments in the study area range from 40 to 285 km in length with offsets of 10 to 300 km.

During February–April 1996 we carried out a 53-day research cruise aboard the R/V *Melville* (Boomerang 06 expedition) [34]. This expedition

involved rock sampling and Seabeam swath coverage along the axis of the SEIR from 88° to 77°E, including approximately 75% coverage out to 0.75 Ma seafloor on and around the ASP plateau. The topographic expression of the spreading axis is often a narrow (<2 km wide) and shallow (<100 m deep) valley, sometimes containing a smaller central ridge or group of circular cones. In some places, particularly on the ASP plateau, the center of the neovolcanic zone (as indicated by strong sidescan sonar reflectivity) is topographically indistinct from the adjacent flanks. Fresh, glassy basalts were recovered from 89 sampling stations between segments F and L (48 dredges and 51 wax cores from F-G-H-I1-I2-J1-J2-J3-J4-K-L). Sampling efforts were concentrated on the ASP plateau, where the average spacing was approximately 10 km between stations.

Major element results for submarine glasses from the region are described in [35,36]. Briefly, 126 chemical groups can be distinguished, based on major element analyses by electron microprobe. MgO ranges between 3.9 and 9.3 wt%, but nine of the eleven ridge segments display a narrow range of less than 2 wt% in MgO. Nearly all glasses are tholeiites or transitional basalts, although there are isolated occurrences of basaltic andesites and Fe–Ti basalts on the ASP plateau, and from an abandoned rift along the southeastern periphery of the plateau (D49-3 from segment J2). On average, glasses from ridge segments on the plateau (I1, I2, J1) have lower Mg# ($Mg^{2+}/[Mg^{2+} + Fe^{2+}]$) and are somewhat more evolved than glasses from off-plateau segments (Table 1). Segment J2, which is partially located in the southeast sector of the plateau, and segment H immediately to the northwest of the plateau, exhibit the least evolved compositions within the study area (ranging up to 8.9 and 9.3 wt% MgO, respectively). Overall, K_2O (0.03–0.98 wt%) and TiO_2 (0.76–3.26 wt%) are roughly correlated in the sample suite, but there appear to be distinct groupings in K_2O behavior as a function of MgO. Notably, segment H lavas display a highly enriched K_2O trend with only a small decrease in MgO (0.03–0.70% K_2O between 9.3 and 7.8% MgO). This trend cannot be simply explained by shallow level crystal fractionation and must reflect melting of variably enriched sub-ridge mantle. MORB glasses from the ASP plateau show trends with somewhat lesser enrichment as MgO decreases, while lavas from ridge segments more distant from the plateau (e.g., F, G, K and L) show shallow sloping trends of K_2O with MgO that are consistent with control by simple crystal fractionation [36].

3. Results

We have analyzed 54 glass samples for $^3He/^4He$ and He concentrations. The sample suite includes 'zero age' glasses from the BMRG 06 expedition, supplemented by glass samples collected in the early 1980s (the French MD37 and Hydro-Amsterdam expeditions), and a glassy rind from a dike exposed along the eastern coast of St. Paul Island (St. Paul #2). Analytical procedures followed methods outlined in [37]. All helium analyses in this study have been performed by crushing in vacuum, liberating helium and associated gases (primarily CO_2) from vesicles trapped within the glass.

High $^3He/^4He$ ratios (9–13.4 R_A) are present atop the ASP plateau (Fig. 2). Such high ratios are usually taken to indicate the presence of a mantle plume derived from a relatively undegassed (deep) source region (although this idea has been challenged [38]). The highest $^3He/^4He$ ratios on the ASP plateau occur at off-axis sites (Fig. 2), consistent with slightly more dilution of plume material beneath the ridge by surrounding MORB mantle. Notably, high $^3He/^4He$ ratios are also found all along segment H, well to the north of the ASP plateau, where values range up to 14.1 R_A. This results in a 'double peak' structure in the regional $^3He/^4He$ distribution (Fig. 2). Peaks in the concentrations of K_2O, P_2O_5 and to a lesser degree TiO_2 can also be seen along the SEIR atop the plateau, and a local Na_8 minimum exists along segment I1 (Fig. 2). The K_2O and P_2O_5 enrichments appear to extend beyond the plateau to include segment H to the north [35]. The high $^3He/^4He$ ratios along segment H and atop the ASP plateau are generally (but not always) accompanied by higher Na_8 and elevated minor element ratios (e.g., K/Ti; [35,36]; Fig. 2).

The $^3He/^4He$ distribution along segment H has a complex structure. All samples along segment H show elevated $^3He/^4He$ ratios, even the few samples with low K/Ti typical of depleted MORB (e.g., K/Ti = 0.03 and 0.08 in samples D73-5 and WC50,

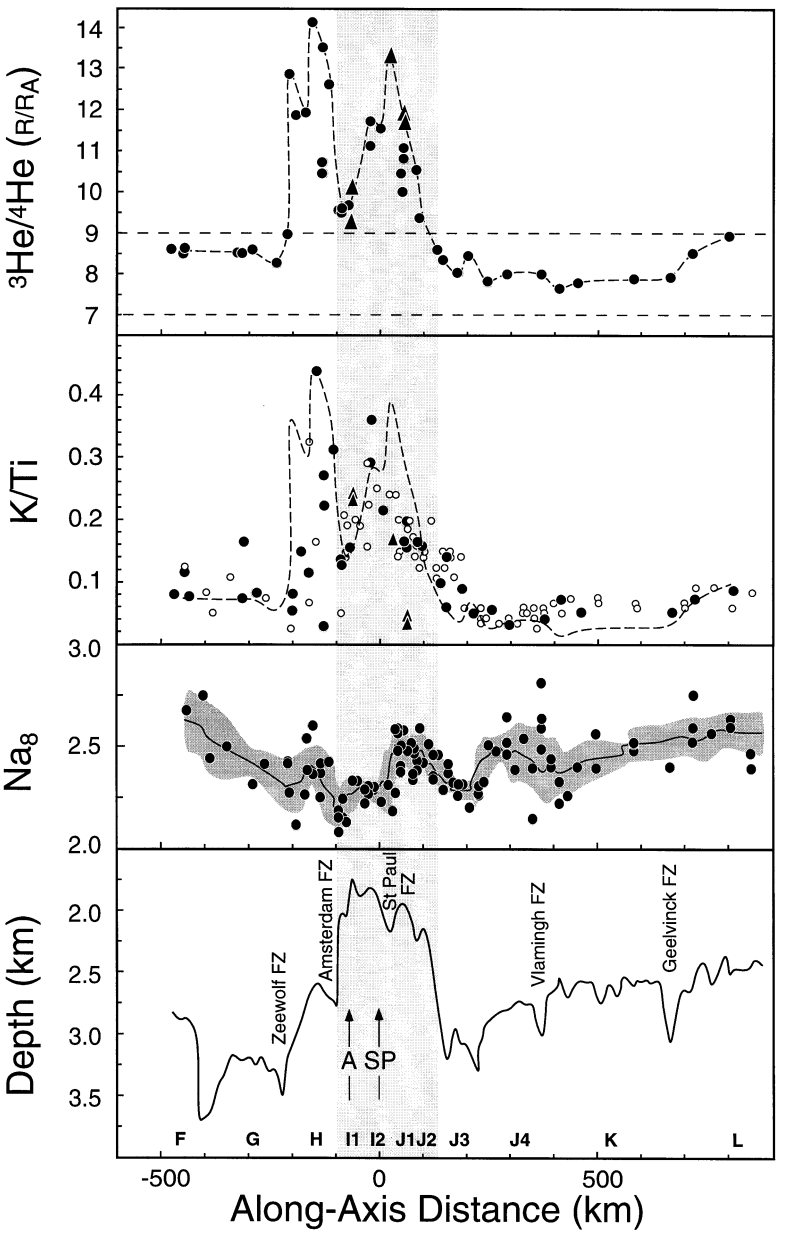

Fig. 2. $^{3}He/^{4}He$ (R/R_A), K/Ti (elemental weight ratio), Na_8 and axial depth (km) vs. distance (in km) along the SEIR, calculated from the pole of plate rotation (13.2ºN, 38.2ºE; [69]) and relative to St. Paul Island (38.70ºS, 77.55ºE). The ASP plateau is shown as a shaded band and extends from −90 km to +140 km. The line for Na_8 is the five-point running mean and the shaded band shows ±1 standard deviation. Filled symbols for K/Ti indicate where the same glass samples have been analyzed for $^{3}He/^{4}He$. Triangles represent lavas from seamounts and off-axis lava fields atop the ASP plateau. The range of 7–9 R_A for normal MORB $^{3}He/^{4}He$ is delineated by a dashed band. The dashed line for K/Ti shows the expected variation for axial lavas (scaled to overlie the data range) if K/Ti and $^{3}He/^{4}He$ covaried perfectly; extremes in the He isotope and K/Ti data are similar in relative amplitude on both long and short length scales.

Table 1
Helium isotope results for Southeast Indian Ridge basalt glasses

Sample	Segment	Depth (m)	Lat. (°S)	Long. (°E)	$^3He/^4He$ (R/R_A)	±	[He] (10^{-6} cm^3 STP/g)	Mg#	K/Ti
BMRG 06									
D34-1	L	2480	41.52	87.09	8.90	0.05	6.21	53.7	0.0883
D36-1	L	2500	41.10	86.23	8.50	0.05	0.88	57.7	0.0745
WC04	K	2953	42.86	83.29	7.89	0.04	3.13	61.0	0.0530
WC07	K	2645	42.35	82.55	7.91	0.04	1.20	60.4	0.0644
WC09	K	2579	41.53	81.47	7.73	0.04	7.62	60.4	0.0531
D39-1	K	2776	41.24	81.15	7.59	0.04	5.52	63.5	0.0735
D41-2	J4	2840	41.77	79.75	7.97	0.04	5.41	63.0	0.0403
D43-2	J4	2785	41.25	79.11	7.98	0.04	2.37	63.5	0.0337
D44-6	J4	2800	40.97	78.79	7.77	0.05	0.47	58.7	0.0612
D46-1	J3	3014	40.75	78.33	8.41	0.04	2.78	63.4	0.0497
D47-6	J3	2845	40.55	78.14	8.03	0.04	4.95	64.0	0.0903
D48-2	J2	2479	39.81	78.39	8.61	0.05	3.21	61.7	0.0984
D54-3	J2	2225	39.45	78.09	9.36	0.05	6.78	53.2	0.161
D49-3*	J2	2543	39.82	78.60	1.19	0.22	0.0045	31.5	0.150
D55-1	J1	2104	39.29	78.18	10.56	0.08	0.31	59.6	0.167
D60-1	J1	1978	38.96	78.11	10.44	0.08	2.12	57.1	0.159
D61-1	J1	2153	38.95	78.13	10.02	0.10	0.093	56.8	0.167
D58-1*	near St.Paul	1370	39.21	77.88	11.71	0.09	0.15	61.0	0.0443
D58-4*	near St.Paul	1370	39.21	77.88	11.93	0.06	0.35	56.8	0.0366
WC34*	near St. Pierre	1378	38.78	77.96	13.41	0.08	0.41	54.0	0.176
D63-1	I2	1838	38.20	78.37	11.57	0.06	4.58	56.6	0.212
D64-2	I2	1805	37.98	78.16	11.11	0.06	0.61	48.3	0.363
D64-8	I2	1805	37.98	78.16	11.72	0.08	0.60	52.4	0.293
D70-1	I1	1850	37.17	78.40	9.63	0.06	1.55	62.4	0.154
WC43	I1	2092	37.12	78.33	9.47	0.05	9.80	57.4	0.146
D71-1	I1	1940	37.06	78.24	9.56	0.06	0.30	50.0	0.130
D71-3	I1	1940	37.06	78.24	9.57	0.05	2.20	52.2	0.139
WC44*	BMRG Smt	875	37.72	77.83	9.28	0.32	0.0074	40.4	0.241
WC45*	BMRG Smt	679	37.72	77.83	10.12	0.06	0.84	48.7	0.241
WC46	H	2734	36.18	78.95	12.63	0.07	2.36	64.9	0.311
D73-3	H	2659	36.07	78.83	13.53	0.07	4.39	61.5	0.272
D73-5	H	2659	36.07	78.83	10.43	0.05	18.6	67.6	0.0295
D73-6	H	2659	36.07	78.83	10.69	0.06	3.01	67.0	0.223
WC47 'h'	H	2840	35.94	78.71	14.13	0.07	3.34	61.9	0.440
WC48	H	2900	35.80	78.59	11.94	0.07	1.66	63.5	0.115
WC49	H	3086	35.64	78.46	11.85	0.06	6.63	61.4	0.150
WC50	H	3413	35.53	78.35	12.86	0.07	1.07	61.1	0.0821
D75-1	Zeewolf FZ	3269	35.28	78.60	8.99	0.05	7.86	62.9	0.0551
D79-1	G	3163	34.57	78.24	8.60	0.05	0.53	64.2	0.0803
D77-2	F	2835	32.95	77.82	8.55	0.04	9.13	61.3	0.0782
D76-2*	F	2178	32.76	77.89	8.49	0.04	7.53	63.4	0.119
MD 37									
03/01 D1-22	B	3625	26.91	72.24	8.26	0.05		65.7	0.125
05/02 D1-3	D	3000	29.70	75.30	8.91	0.07		58.2	0.0830
05/03 D1-6	D	4100	29.81	75.18	8.77	0.07		61.1	0.0830
07/04 D1-2	F	2700	32.67	77.62	8.58	0.06		59.8	0.0813
22/07 D1-1	G	3080	34.38	78.02	8.51	0.05		61.6	0.166
22/07 D2-3	G	3100	34.35	78.01	8.53	0.07		63.8	0.0764
18/06 D2-3	J1	2320	38.98	78.14	10.78	0.08		52.4	0.158
18/06 D3-3	J1	2020	38.96	78.16	11.07	0.06		54.0	0.199
13/05 D1-5	J3	3400	40.36	77.89	8.31	0.05		58.4	0.0606

Table 1 (continued)

Sample	Segment	Depth (m)	Lat. (°S)	Long. (°E)	$^3He/^4He$ (R/R_A)	±	[He] (10^{-6} cm^3 STP/g)	Mg#	K/Ti
Hydro-Amsterdam									
D3-5	I2	2100	37.52	78.43	1.43	0.15	0.0044	36.3	0.108
D4-3	G	3700	34.91	78.67	8.25	0.04	14.6	64.8	0.224
St. Paul #2	–	0	38.70	77.55	1.69	0.32	0.0044	37.7	0.232

Samples were recovered by the Boomerang 06 (R/V *Melville*) MD37 (*Marion Dufresne*) and Hydro-Amsterdam (*Jean Charcot*) expeditions. He isotope analyses were performed by in vacuo crushing of hand-picked glasses, as described elsewhere [37]. ± values are 2 standard errors, computed as the quadrature sum of uncertainties associated with blank, sample and air standard analyses. Major and minor element results from [36], determined by electron microprobe. Mg# = $Mg^{2+}/(Mg^{2+} + Fe^{2+})$ assuming $Fe^{3+}/Fe^{2+} = 0.15$.
Asterisk indicates BMRG06 samples from young volcanic edifices (WC44, 45), or from young off-axis lava fields targeted from sidescan reflectivity (WC34, D58 and D76). D49 is from the tip of a large abandoned rift. All other BMRG samples are from within the neovolcanic zone of the SEIR. Most of the MD37 and Hydro-Amsterdam samples appear to have been collected from slightly off-axis based on the multi-beam swath mapping carried out during BMRG06.

respectively; Fig. 2). This indicates the extreme sensitivity of the $^3He/^4He$ ratio to the introduction of plume material into the sub-ridge mantle of this region. The $^3He/^4He$ ratio increases with K/Ti, both along segment H in particular, and throughout the region in general (Fig. 3), and the highest $^3He/^4He$ (14.1 R_A) occurs in the most enriched sample (WC47; K/Ti = 0.45). There is also a large variability in major element composition and $^3He/^4He$ at a single locality along segment H; for example, within dredge 73 the $^3He/^4He$ and K/Ti ranges are 10.4–13.5 R_A and 0.03–0.27, respectively. This variability indicates that there is also a significant short-range spatial, and perhaps temporal, variability in magma types along some parts of segment H. Lastly, high $^3He/^4He$ ratios along segment H per-

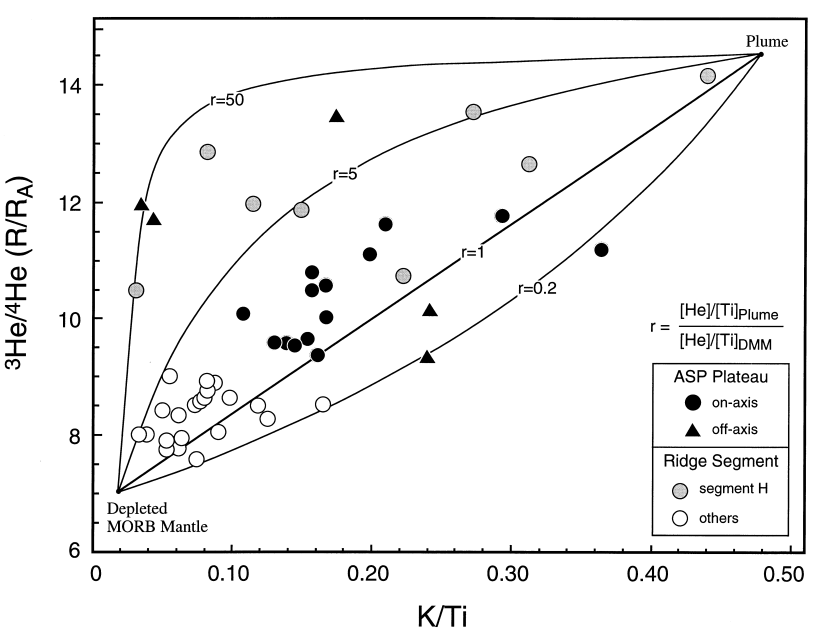

Fig. 3. $^3He/^4He$ vs. K/Ti for basalt glasses from the Southeast Indian Ridge. r is the abundance ratio of He/Ti in the plume source relative to that in the MORB mantle source [70]. If binary mixing is applicable, segment H lavas require higher, and more variable, r values (r = 1–50) than axial lavas from the ASP plateau (r = 0.2–2). See text for further discussion.

sist all the way to its intersection with segment G at the Zeewolf transform (Fig. 2). Just beyond that point (e.g., in sample D75-1 collected from a short intra-transform spreading center) the $^3He/^4He$ drops to normal MORB values (7–9 R_A). Although the sampling density is sparse beyond segments F and G, normal MORB values of 7 to 9 R_A appear to continue all the way to the Rodrigues Triple Junction, as evidenced by the MD37 results north of 30°S (Table 1).

A single sample (D49-3) from the tip of an abandoned rift along segment J2 on the southeast flank of the ASP plateau was analyzed for He isotopes. It shows a very low $^3He/^4He$ ratio (1.2 ± 0.2 R_A) accompanied by very low He content (4.5×10^{-9} cm^3/g). Sample 49-3 is a Fe–Ti basalt which apparently underwent significant gas loss during its evolution and/or eruption. This glass sample has a very high Cl content (1100 ppm; [36]), indicating that gas loss was accompanied by contamination with a seawater-derived component, probably through assimilation of hydrothermally altered wallrock. Such low $^3He/^4He$ ratios are not common along ocean spreading centers, but they are sometimes found in evolved lavas erupted close to transform faults, at overlapping spreading centers and from propagating rifts ([39,40] and D.W. Graham, unpubl. results). This is further supported by the low $^3He/^4He$ ratios, near the atmospheric ratio, for the sample JC D3-5 from the plateau region, and for the dike margin glass taken from St. Paul Island (Table 1). Both of these are differentiated Fe–Ti basalts (Mg# = 36 with $FeO^* > 14\%$), and each has a low He content identical to that found in sample 49-3, which was dredged from below 2500 m water depth. These results suggest that atmospheric $^3He/^4He$ ratios and trapped He contents of $\sim 4.5 \times 10^{-9}$ cm^3/g may be a common feature of highly evolved and degassed basalt glasses. The $^3He/^4He$ ratios of these three evolved samples have obviously been modified by crustal processes, and they provide no information on mantle source composition.

All other ridge segments, excluding those on the ASP plateau (I1, I2, J1, J2) and segment H to the northwest, show $^3He/^4He$ values between 7 and 9 R_A, typical of MORB. There may be a large-scale spatial structure to these normal MORB helium isotope ratios away from the plateau (Fig. 2). Basalts from segments F and G to the northwest have $^3He/^4He$ ratios between 8.3 and 9.0 R_A, while segments K and J4 to the southeast show the lowest $^3He/^4He$ ratios in the region and range between 7.6 and 8.0 R_A. Thus, as one transects across the ASP plateau, there is a decrease from the northwest to the southeast in the MORB 'background' $^3He/^4He$ values to either side of the high $^3He/^4He$ influence. Slightly higher $^3He/^4He$ ratios may also be present to either side of the J4–K segments in the southeast, because ratios on segment J3 are 8.0 to 8.4 R_A ($n = 3$) while those along segment L are 8.5 and 9.0 R_A. Due to the sparse sampling on these latter ridge segments, however, we do not feel we can make comparisons of their inter-segment variability as confidently as elsewhere.

4. Discussion

4.1. Plume flow and mantle melting

The presence of high $^3He/^4He$ ratios on the ASP plateau is strong evidence that the ASP mantle plume is derived from a high $^3He/^4He$ source region. This hotspot mantle source has $^3He/^4He$ ratios significantly higher than those of the mantle source(s) for Indian Ocean MORB, and presumably lies at greater depths than the MORB source. The high $^3He/^4He$ ratios on segment H to the north, along the part of the SEIR that forms a U-shaped deviation toward the ASP plateau (Fig. 1), also indicate that the ASP plume supplies an approximately northward flow into the sub-ridge mantle beneath this region of the SEIR. The elevated $^3He/^4He$ signal extends well north of the plateau, indicating that this northward mantle flow must be sufficiently deep that it is not impeded by any contrast in lithospheric thickness which might exist across the Amsterdam Fracture Zone. Given that the base of the lithosphere must slope upward from beneath St. Paul and Amsterdam islands toward the ridge segments I1, I2 and H, it seems likely that any lithospheric thickening near the northern margin of the plateau could serve to guide upwelling hotspot material to the north and northeast.

High $^3He/^4He$ ratios are found along the entire length of segment H right up to its intersection with

the Zeewolf transform, and then they abruptly drop to normal MORB values beyond this intersection. Within the Zeewolf transform, glassy basalts were recovered from a short spreading ridge (D75), and show a normal MORB $^3He/^4He$ ratio of 9.0 R_A. This latter observation suggests that flow of ASP plume material beneath the northern end of segment H must be occurring at a shallow depth, perhaps even confined to depths within the region of melt extraction beneath the ridge. Once this flow reaches the Zeewolf transform, it appears to be so thin that it is dammed against older lithosphere adjacent to the Zeewolf transform.

Narrow $^3He/^4He$ spikes, relative to those for other isotopic tracers such as Sr and Nd, have been reported from 17°S on the East Pacific Rise [41]. This observation has been attributed to the extreme sensitivity of the helium concentration in the residual mantle to the history of partial melting. This potentially allows a further test of shallow vs. deep mantle flow, because if He is 'mined' by an early (deeper) stage of melting in the plume stem prior to lateral flow of plume material toward the spreading ridge, then a stronger plume He signature could be found along ridge segments supplied by the outer, less extensively melted portions of the plume. There is evidence for this effect along ridge sections influenced by the Easter [5,42] and St. Helena [14] hotspots. In those cases, the mixing systematics between He isotopes and those of Sr and Pb indicate that, where the center of plume feeds the ridge and the isotopic anomaly is strong, lower He/Pb and He/Sr ratios are present in the plume end-member compared to ridge sections where peripheral parts of the plume are involved. These lower He/Pb and He/Sr ratios have been suggested to result from melting effects beneath the hotspot. The end result is that the sensitivity of the respective isotope tracers to plume material can be affected by earlier stages of melt removal.

Some of the segment H lavas are quite similar in their $^3He/^4He$–K/Ti relationships to off-axis lavas from the ASP plateau (Fig. 3). These $^3He/^4He$–K/Ti relations are consistent with tapping of the outer portions of the ASP plume by the segment H mantle. These outer portions of the plume have not undergone the same degree of processing (melting?) as plume material derived from the hotter plume center that ultimately contaminates the sub-ridge mantle beneath the ASP plateau. Off-axis sites from the plateau also show variable $^3He/^4He$–K/Ti characteristics, so varying extents of melting due to local variations in lithospheric thickness [43] may also be important.

Given that varying degrees of melt extraction across the plume stem may have occurred, the sense of $^3He/^4He$–K/Ti displacement of the segment H lavas in Fig. 3 relative to axial lavas from the ASP plateau may be explained by binary mixing. This mixing would occur between a common MORB mantle end-member having only a narrow range of $^3He/^4He$, K/Ti and He/Ti ratios, and a plume end-member with a narrow range of $^3He/^4He$ and K/Ti ratios. The plume material influencing the respective ridge segments appears, however, to have a variable He/Ti ratio that is related to geographic position (e.g., segment H vs. ridge segments I1, I2 and J1 atop the ASP plateau; see Fig. 3). This variable He/Ti ratio may depend on the lateral position within the plume from which it was derived, and be related to the prior melt extraction history. MORB mantle that is more strongly influenced by material derived from the hotter plume center would likely show a larger degree of melting, and produce lavas having slightly lower Na_8. (Na_8 is the Na_2O content corrected for crystal fractionation to 8 wt% MgO, and varies inversely in MORB glasses with the extent of melting beneath ridges [44]). Based on the local minimum in Na_8 along the ridge axis atop the plateau and opposite Amsterdam Island (Fig. 2), the plume center would therefore be close to the position of Amsterdam Island and adjacent to segment I1. During upslope flow of plume mantle along the base of the lithosphere towards a spreading ridge, pressure release melting may also continue. These melt extraction processes could eventually lead to a supply of incompatible-element depleted plume material to the nearby sub-ridge mantle [10]. Consequently, the plume mantle feeding segment H and segments on the ASP plateau (I1, I2 and J1) may have experienced different extents of He/Ti fractionation. Assuming He is more incompatible than Ti during partial melting (e.g., [45]) this points to a stronger melt depletion in the plume material supplying the ASP segments, and implicates the somewhat cooler, less melted outer portions of the plume for feeding the

segment H mantle. Melting, rather than degassing, is implicated because of the generally sympathetic variations in K/Ti and $^{3}He/^{4}He$ (Fig. 2). A peak in $^{3}He/^{4}He$ therefore occurs where there is a maximum in plume He contribution, and this is not necessarily the same as a maximum in plume mass fraction.

Morgan [46] hypothesized that the ASP hotspot has a secondary origin, created by mantle melting during channeled flow of Kerguelen plume material toward the ridge axis. However, the Pb, Sr and Nd isotope compositions of Amsterdam and St. Paul Island lavas (e.g., $^{206}Pb/^{206}Pb = 18.7–19.1$, $^{87}Sr/^{86}Sr = 0.7034–0.7039$) are very distinct from those at Kerguelen (e.g., $^{206}Pb/^{206}Pb = 17.5–18.7$, $^{87}Sr/^{86}Sr = 0.7043–0.7060$) [21,47–56], evidence that the ASP hotspot is a separate hotspot with a significantly smaller mass flux. Nevertheless, Kerguelen may still exert some influence on the composition of SEIR basalts, either through radial contamination of the upper mantle, or through some form of channeled flow. The presence of gravity lineations and a broad chain of seamounts trending from the Kerguelen plateau toward the southeastern part of the ASP plateau could be taken to suggest an active plume–ridge connection between the Kerguelen hotspot and the SEIR near this region [32]. A pronounced Kerguelen-like isotopic signature was previously reported for a few MORB glasses along segment J1 near its intersection with the Hillegom transform [20–22] (the active transform domain which is co-linear with the St. Paul FZ). Two of those MORB glasses analyzed in this study (MD37 18/06 D2 and D3; Table 1) show elevated $^{3}He/^{4}He$ ratios ($\sim 11\ R_A$), and a nearby off-axis lava (WC34) has the highest $^{3}He/^{4}He$ on the ASP plateau. It is important to point out the limited extent of this Kerguelen-like isotope signature; based on the available Sr–Nd–Pb isotope data [20,21], it does not appear to be present on the nearby segments I2 or J3.

Several explanations are possible for this Kerguelen-like Sr–Nd–Pb isotope signature and the coexisting high $^{3}He/^{4}He$ ratios. One simple explanation is that there is an active hotspot–ridge connection between Kerguelen and the SEIR, and that the Kerguelen plume end-member has a high $^{3}He/^{4}He$ ratio. High $^{3}He/^{4}He$ ratios, up to 12.3 R_A, have been observed in two ultramafic xenoliths from Kerguelen [57], although most samples studied to date from there have MORB-like or lower $^{3}He/^{4}He$ values [57,58]. High $^{3}He/^{4}He$ ratios, up to 18 R_A, are found at Heard Island much farther to the south on the Kerguelen plateau [59], but those lavas display a very wide range of Sr, Nd and Pb isotope compositions [54,55], making it difficult to characterize that plume end-member by any single set of isotopic values. A second explanation is that some small amount of Kerguelen hotspot material has been entrained into the edge of the ASP plume as it ascends through the upper mantle and is swept to the north. Although very speculative, maybe the Kerguelen hotspot material ultimately reaching the ASP plateau is a mantle residue of some melt removal. If this material is then invaded locally by a small amount of He-rich ASP plume material, it might retain its Sr–Nd–Pb isotopic character but acquire elevated $^{3}He/^{4}He$ ratios. A third explanation is that the Kerguelen-like isotope signature on the ASP plateau is due to inherent heterogeneity within the ASP plume. Although this requires a very large range in isotope composition at a single locality, it has been seen over relatively short distances at a few ocean islands previously [60], including Heard Island [54,55]. In this case, the isotope composition seen at Amsterdam and St. Paul (e.g., $^{206}Pb/^{206}Pb \approx 19$, $^{87}Sr/^{86}Sr \approx 0.7035$) may be viewed as representing the common plume component described by Hanan and Graham [18].

4.2. Helium isotopes in the Indian Ocean and the history of mantle mixing

Away from the ASP plateau, the SEIR MORB glasses show a He isotope range comparable to MORB from the Atlantic and Pacific Oceans (7–9 R_A), despite their systematically different Pb and Sr isotope compositions in such a global comparison [20–23]. This indicates that while lower $^{3}He/^{4}He$ ratios may sometimes be associated with the enriched Pb–Nd–Sr isotopic signatures shown by some Indian Ocean MORB, such as in the AAD region [61], such lower values are not a basin-wide characteristic of the Indian Ocean.

Convective mixing in the mantle serves to reduce isotopic and compositional heterogeneities to small blobs and strings of distinct material [62,63]. In the solid state this material remains essentially unmixed on a time scale which depends on the strain rate

of the mantle. Eventually the injected material will be thinned to a point when homogenization with surrounding mantle peridotite will occur by diffusion. Partial melting acts as a 'filter' to obscure the shorter length scales of mantle heterogeneity as deduced from isotope variations in basalts, but larger-scale variations (>1 km) in source composition can be clearly discerned. The pervasive Pb–Sr–Nd isotopic shift of Indian MORBs relative to those of the Atlantic and Pacific [64,65] has been attributed to several different causes: (1) contamination of the asthenosphere by broad dispersion of Kerguelen hotspot material [26]; (2) breakup and entrainment of Gondwana lithosphere into the upper mantle [66,67]; or (3) the presence of small amounts of recycled sediment in the MORB mantle source [68]. Regardless of the model chosen to explain the Indian MORB isotopic features, stirring in the Indian MORB mantle must have been so thorough that only normal MORB $^3He/^4He$ ratios (7–9 R_A) are now observed along sections of the SEIR away from the ASP plateau. In this context, this 'background' helium isotope signal appears to decrease along the SEIR across the ASP plateau from northwest to southeast (Fig. 2). Basalts from segments F and G to the northwest of the ASP plateau have higher $^3He/^4He$ ratios (8.3–9.0 R_A; $n = 8$) than those from segments K and J4 to the southeast (7.6–8.0 R_A; $n = 7$). Based on the gravity lineations that trend obliquely into the ridge from the south, segments K and J4 were suggested by Small [32] to be candidate localities influenced by the Kerguelen plume. These segments may, therefore, also be viewed as showing a localized and weak depression of $^3He/^4He$ ratio (Fig. 2) relative to segment J3 (8.0–8.4 R_A; $n = 3$) and segment L (8.5–8.9 R_A; $n = 2$) on either side. Thus, two alternative explanations appear to be possible given the present He isotope data set. Either the helium isotope variations in this part of the study area may be due to a channeled influence of a Kerguelen 'low $^3He/^4He$' plume component toward segments K and J4, or they may be due to a changing 'background $^3He/^4He$' from north to south across the ASP plateau, produced by an earlier, broad contamination of the asthenosphere from a low $^3He/^4He$ plume component.

Hotspot–ridge interaction in this region of the SEIR most likely involved (at least) a two-stage process. In the first stage, widespread dispersion of Kerguelen plume material may have occurred, prior to, or contemporaneous with, the opening of the ocean basin (>38 Ma [26,52]). This same MORB mantle would have been polluted again by the ASP hotspot more recently. If ridge segments can now be identified which show only a memory of the first stage of pollution (for example, if binary mixing accounts for the Pb–Sr–Nd isotope systematics along some sections of the SEIR), then in principle the scale of blobs remaining from the first stage of pollution may be deduced. A second possibility is that stirring/mixing in the upper mantle has reduced those original heterogeneities to a scale which is too small to be discretely sampled by recent melting. However, the second stage of hotspot–ridge interaction between variably polluted asthenosphere and ASP hotspot material would still be observable. In this case the extent of earlier asthenosphere pollution should decrease radially from the original site of plume dispersal. This second scenario is analogous to that for the South Atlantic MORB [3,14]. In the South Atlantic, isotopic anomalies along the ridge reveal that ongoing hotspot–ridge interaction is superposed on a systematically varying, depleted 'background'. This background variation results from an earlier, radial dispersion of plume material into the upper mantle when the hotspots were intraplate, prior to continental breakup. How the background pollution of the MORB mantle changes along the Southeast Indian Ridge, and the scale of any isotopic heterogeneities possibly remaining from earlier plume dispersal, may be assessed in the future from the results of a Pb–Sr–Nd comparative isotope study for this same suite of SEIR glasses.

5. Conclusions

Helium isotope variations along the Southeast Indian Ridge near the Amsterdam and St. Paul islands reveal the presence of an active mantle plume and the nature of shallow mantle flow in the region. The Amsterdam–St. Paul plume source has $^3He/^4He > 14\ R_A$, evidence for derivation from a mantle reservoir located deeper than the upper mantle source for mid-ocean ridge basalts. The He isotopes show systematic variations with other chemical parameters

such as K/Ti. High $^3He/^4He$ ratios also occur along a ridge segment located well to the north of the ASP plateau. These variations suggest that the ASP mantle plume supplies a north-northeastward mantle flow beneath this section of the Southeast Indian Ridge. High $^3He/^4He$ ratios are also found in lavas atop the ASP plateau having a Sr, Nd and Pb isotopic signature resembling Kerguelen. The $^3He/^4He$ ratios for MORB erupted farther away from the ASP plateau show a systematic decrease moving from northwest to southeast. This 'background' MORB variation may reflect a widespread contamination of the asthenosphere by the Kerguelen hotspot at an earlier time, or the localized input of some Kerguelen plume material along ridge segments to the southeast of the ASP plateau. Each of these explanations implies that the portions of the Kerguelen plume that may have influenced this region had relatively low $^3He/^4He$ ratios ($<8\ R_A$).

Acknowledgements

We thank Dan Scheirer and Don Forsyth for excellent and timely handling of the shipboard geophysical data, and the Captain Eric Buck and the crew of the R/V *Melville* for a highly successful and memorable cruise. Bernard Dupré and Laure Dosso kindly provided the MD37 and Charcot and St. Paul glass samples, respectively. Bill White, Tim Elliott and an anonymous reviewer provided constructive and insightful reviews. Barry Hanan and Brennan Jordan provided helpful comments on the manuscript. We thank the Terres Australes et Antarctiques Françaises (TAAF) for their clearance to work in territorial waters around the Amsterdam and St. Paul islands. This work was supported by grants 8911505 and 9417553 from the Ocean Sciences Division of NSF. ***[FA]***

References

[1] J.-G. Schilling, Iceland mantle plume: geochemical evidence along Reykjanes Ridge, Nature 242 (1973) 565–571.

[2] J.-G. Schilling, R.H. Kingsley, J.D. Devine, Galapagos hot spot–spreading center system 1, spatial, petrological and geochemical variations (83ºW–101ºW), J. Geophys. Res. 87 (1982) 5593–5610.

[3] B.B. Hanan, R.H. Kingsley, J.-G. Schilling, Pb isotope evidence in the South Atlantic for migrating ridge–hotspot interactions, Nature 322 (1986) 137–144.

[4] B.B. Hanan, J.-G. Schilling, Easter microplate evolution: Pb isotope evidence, J. Geophys. Res. 94 (1989) 7432–7448.

[5] R.J. Poreda, J.-G. Schilling, H. Craig, Helium isotope ratios in Easter Microplate basalts, Earth Planet. Sci. Lett. 119 (1993) 319–329.

[6] R. Kingsley, J.-G. Schilling, Plume–ridge interaction in the Easter–Salas y Gomez seamount chain–Easter microplate system: Pb isotope evidence, J. Geophys. Res. 103 (1998) 24159–24177.

[7] M.A. Feighner, M.A. Richards, The fluid dynamics of plume–ridge and plume–plate interactions: an experimental investigation, Earth Planet. Sci. Lett. 129 (1995) 71–182.

[8] C. Kincaid, J.-G. Schilling, C. Gable, The dynamics of off-axis plume–ridge interaction in the uppermost mantle, Earth Planet. Sci. Lett. 137 (1996) 29–43.

[9] N.M. Ribe, The dynamics of plume–ridge interaction 2, Off-ridge plumes, J. Geophys. Res. 101 (1996) 16195–16204.

[10] N.H. Sleep, Lateral flow of hot plume material ponded at sublithospheric depths, J. Geophys. Res. 101 (1996) 28065–28083.

[11] G. Ito, J. Lin, C.W. Gable, Interaction of mantle plumes and migrating midocean ridges: implications for the Galápagos plume–ridge system, J. Geophys. Res. 102 (1997) 15403–15417.

[12] M.D. Kurz, W.J. Jenkins, J.-G. Schilling, S.R. Hart, Helium isotopic variations in the mantle beneath the central North Atlantic Ocean, Earth Planet. Sci. Lett. 58 (1982) 1–14.

[13] R.J. Poreda, J.-G. Schilling, H. Craig, Helium and hydrogen isotopes in ocean-ridge basalts north and south of Iceland, Earth Planet. Sci. Lett. 78 (1986) 1–17.

[14] D.W. Graham, W.J. Jenkins, J.-G. Schilling, G. Thompson, M.D. Kurz, S.E. Humphris, Helium isotope geochemistry of mid-ocean ridge basalts from the South Atlantic, Earth Planet. Sci. Lett. 110 (1992) 133–147.

[15] M. Moreira, T. Staudacher, P. Sarda, J.-G. Schilling, C.J. Allègre, A primitive plume neon component in MORB: the Shona ridge-anomaly, South Atlantic (51–52ºS), Earth Planet. Sci. Lett. 133 (1995) 367–377.

[16] J.E. Lupton, D.W. Graham, J.R. Delaney, H.P. Johnson, Helium isotope variations in Juan de Fuca Ridge basalts, Geophys. Res. Lett. 20 (1993) 1851–1854.

[17] E. Ito, W.M. White, C. Göpel, The O, Sr, Nd and Pb isotope geochemistry of MORB, Chem. Geol. 62 (1987) 157–176.

[18] B.B. Hanan, D.W. Graham, Lead and helium isotope evidence from oceanic basalts for a common deep source of mantle plumes, Science 272 (1996) 991–995.

[19] J.J. Mahoney, J.H. Natland, W.M. White, R. Poreda, S.H. Bloomer, R.L. Fisher, A.N. Baxter, Isotopic and geochemical provinces of the western Indian Ocean spreading centers, J. Geophys. Res. 94 (1989) 4033–4052.

[20] B. Hamelin, B. Dupré, C.-J. Allègre, Pb–Sr–Nd isotopic data of Indian Ocean ridges: new evidence of large-scale

mapping of mantle heterogeneities, Earth Planet. Sci. Lett. 76 (1986) 288–298.
[21] L. Dosso, H. Bougault, P. Beuzart, J.-Y. Calvez, J.-L. Joron, The geochemical structure of the South-East Indian Ridge, Earth Planet. Sci. Lett. 88 (1988) 47–59.
[22] A. Michard, R. Montigny, R. Schlich, Geochemistry of the mantle beneath the Rodriguez triple junction and the South-East Indian Ridge, Earth Planet. Sci. Lett. 78 (1986) 104–114.
[23] R.C. Price, A.C. Kennedy, M. Riggs-Sneeringer, F.A. Frey, Geochemistry of basalts from the Indian Ocean triple junction: implications for the generation and evolution of Indian Ocean basalts, Earth Planet. Sci. Lett. 78 (1986) 379–396.
[24] R.A. Duncan, Hotspots in the southern oceans: an absolute frame of reference motion of the Gondwana continent, Tectonophysics 74 (1981) 29–42.
[25] J.-G. Schilling, Fluxes and excess temperatures of mantle plumes inferred from their interaction with migrating ridges, Nature 352 (1991) 397–403.
[26] M. Storey, A.D. Saunders, J. Tarney, I.L. Gibson, M.J. Norry, M.F. Thirlwall, P. Leat, R.N. Thompson, M.A. Menzies, Contamination of the Indian Ocean asthenosphere by the Kerguelen–Heard mantle plume, Nature 338 (1989) 574–576.
[27] J.-Y. Royer, M.F. Coffin, Jurassic to Eocene plate tectonic reconstructions in the Kerguelen Plateau region, Proc. ODP, Sci. Results 120 (1978) 917–928.
[28] J.-Y. Royer, D.T. Sandwell, Evolution of the eastern Indian Ocean since the Late Cretaceous: constraints from Geosat altimetry, J. Geophys. Res. 94 (1989) 13755–13782.
[29] R.A. Duncan, M. Storey, The life cycle of Indian Ocean hotspots, AGU, Geophys. Monogr. 70 (1992) 91–103.
[30] B.P. Luyendyk, W. Rennick, Tectonic history of aseismic ridges in the eastern Indian Ocean, Geol. Soc. Am. Bull. 88 (1977) 1347–1356.
[31] D.T. Sandwell, W.H. Smith, Marine gravity anomaly from satellite altimetry, $34'' \times 53''$ poster, Scripps Institution of Oceanography, Geological Data Center, La Jolla, CA, 1995.
[32] C. Small, Observations of ridge–hotspot interactions in the Southern Ocean, J. Geophys. Res. 100 (1995) 17931–17946.
[33] J.-Y. Royer, R. Schlich, Southeast Indian Ridge between the Rodriguez Triple Junction and the Amsterdam and Saint-Paul Islands: detailed kinematics for the past 20 m.y, J. Geophys. Res. 93 (1988) 13524–13550.
[34] D. Scheirer, D. Forsyth, K. Johnson, D. Graham, The Southeast Indian Ridge near Amsterdam and St. Paul Islands: results from Boomerang Leg 6, Ridge Events 7 (1996) 5–9.
[35] L.M. Douglas, D.W. Graham, K.T.M. Johnson, D.S. Scheirer, D.W. Forsyth, Variations in major element composition of basalt glasses along the Southeast Indian Ridge in the vicinity of the Amsterdam–Saint Paul Platform, EOS 77 (1996) F690.
[36] L.M. Douglas Priebe, Geochemical and Petrogenetic Effects of the Interaction of the Southeast Indian Ridge and the Amsterdam–St. Paul Hotspot, M.S., Oregon State University, 1998.
[37] D.W. Graham, L.M. Larsen, B.B. Hanan, M. Storey, A.K. Pedersen, J.E. Lupton, Helium isotope composition of the early Iceland mantle plume inferred from the Tertiary picrites of West Greenland, Earth Planet. Sci. Lett. 160 (1998) 241–255.
[38] D.L. Anderson, The helium paradoxes, Proc. Natl. Acad. Sci. 95 (1998) 4822–4827.
[39] D.W. Graham, M.D. Kurz, W.J. Jenkins, G. Thompson, R. Batiza, Constraints on basaltic magma evolution inferred from He isotope geochemistry of Pacific seamounts and overlapping spreading centers, EOS 66 (1985) 1120.
[40] D.L. Hilton, K. Hammerschmidt, G. Loock, H. Friedrichsen, Helium and argon isotope systematics of the central Lau Basin and Valu Fa Ridge: evidence of crust/mantle interactions in a back-arc basin, Geochim. Cosmochim. Acta 57 (1993) 2819–2841.
[41] J.J. Mahoney, J.M. Sinton, M.D. Kurz, J.D. Macdougall, K.J. Spencer, G.W. Lugmair, Isotope and trace element characteristics of a super-fast spreading ridge: East Pacific Rise, 13– 23ºS, Earth Planet. Sci. Lett. 121 (1993) 173–193.
[42] K. Rubin, J. Mahoney, What's on the plume channel?, Nature 362 (1993) 109–110.
[43] R.M. Ellam, Lithospheric thickness as a control on basalt geochemistry, Geology 20 (1992) 153–156.
[44] E.M. Klein, C.H. Langmuir, Global correlations of ocean ridge basalt chemistry with axial depth and crustal thickness, J. Geophys. Res. 92 (1987) 8089–8115.
[45] B. Marty, P. Lussiez, Constraints on rare gas partition coefficients from analysis of olivine-glass from a picritic mid-ocean ridge basalt, Chem. Geol. 106 (1993) 1–7.
[46] W.J. Morgan, Rodriguez, Darwin, Amsterdam,.., a second type of hotspot island, J. Geophys. Res. 83 (1978) 5355–5360.
[47] W.M. White, Sources of oceanic basalts: radiogenic isotopic evidence, Geology 13 (1985) 115–118.
[48] L. Dosso, P. Vidal, J.M. Cantagrel, J. Lameyre, A. Marot, S. Zimine, 'Kerguelen: continental fragment or oceanic island?' petrology and isotopic geochemistry evidence, Earth Planet. Sci. Lett. 43 (1979) 46–60.
[49] L. Dosso, V.R. Murthy, A Nd isotopic study of the Kerguelen islands: inferences on enriched mantle sources, Earth Planet. Sci. Lett. 48 (1980) 268–276.
[50] M. Storey, A.D. Saunders, J. Tarney, P. Leat, M.F. Thirlwall, R.N. Thompson, M.A. Menzies, G.F. Marriner, Geochemical evidence for plume–mantle interactions beneath Kerguelen and Heard Islands, Indian Ocean, Nature 336 (1988) 371–374.
[51] D. Weis, Y. Bassias, I. Gautier, J.-P. Mennessier, Dupal anomaly in existence 115 Ma ago: evidence from isotopic study of the Kerguelen Plateau (South Indian Ocean), Geochim. Cosmochim. Acta 53 (1989) 2125–2131.
[52] D. Weis, W.M. White, F.A. Frey, R.A. Duncan, M.R. Fisk, J. Dehn, J. Ludden, A. Saunders, M. Storey, The influence

of mantle plumes in generation of Indian oceanic crust, AGU, Geophys. Monogr. 70 (1992) 57–89.
[53] D. Weis, F.A. Frey, H. Leyrit, I. Gautier, Kerguelen Archipelago revisited: geochemical and isotopic study of the southeast province lavas, Earth Planet. Sci. Lett. 118 (1993) 101–119.
[54] J. Barling, S.L. Goldstein, Extreme isotope variations in Heard Island lavas and the nature of mantle reservoirs, Nature 348 (1990) 59–62.
[55] J. Barling, S.L. Goldstein, I.A. Nicholls, Geochemistry of Heard Island (Southern Indian Ocean): characterization of an enriched mantle component and implications for enrichment of the sub-Indian ocean mantle, J. Petrol. 35 (1994) 1017–1053.
[56] J.J. Mahoney, W. Jones, F.A. Frey, V. Salters, D.G. Pyle, H. Davies, Geochemical characteristics of lavas from Broken Ridge, the Naturaliste Plateau and southernmost Kerguelen Plateau: Cretaceous volcanism in the southeast Indian Ocean, Chem. Geol. 120 (1995) 315–345.
[57] P.J. Valbracht, M. Honda, T. Matsumoto, N. Mattielli, I. McDougall, R. Ragettli, D. Weis, Helium, neon and argon isotope systematics in Kerguelen ultramafic xenoliths: implications for mantle source signatures, Earth Planet. Sci. Lett. 138 (1996) 29–38.
[58] D. Vance, J.O.H. Stone, R.K. O'Nions, He, Sr, and Nd isotopes in xenoliths from Hawaii and other oceanic islands, Earth Planet. Sci. Lett. 96 (1989) 147–160.
[59] D.R. Hilton, J. Barling, G.E. Wheller, Effect of shallow-level contamination on the helium isotope systematics of ocean-island lavas, Nature 373 (1995) 330–333.
[60] J.D. Woodhead, M.T. McCulloch, Ancient seafloor signals in Pitcairn Island lavas and evidence for large amplitude, small length-scale mantle heterogeneities, Earth Planet. Sci. Lett. 94 (1989) 257–273.
[61] D. Graham, J. Lupton, E. Klein, D. Christie, D. Pyle, Helium isotope geochemistry of the Australian–Antarctic Discordance, 7th Int. Conf. Geochronology, Cosmochronology and Isotope Geology, Geol. Soc. Aust. 27 (1990) 41.
[62] M. Gurnis, Stirring and mixing in the mantle by plate-scale flow: large persistent blobs and long tendrils coexist, Geophys. Res. Lett. 13 (1986) 1474–1477.
[63] C.J. Allègre, D.L. Turcotte, Implications of a two-component marble-cake mantle, Nature 323 (1986) 123–127.
[64] B. Dupré, C.J. Allègre, Pb–Sr isotope variation in Indian Ocean basalts and mixing phenomena, Nature 303 (1983) 142–146.
[65] S.R. Hart, A large-scale isotope anomaly in the Southern Hemisphere mantle, Nature 309 (1984) 753–757.
[66] J. Mahoney, A.P. Le Roex, Z. Peng, R.L. Fisher, J.H. Natland, Southwestern limits of Indian Ocean Ridge mantle and the origin of low $^{206}Pb/^{204}Pb$ mid-ocean ridge basalt: isotope systematics of the Central Southwest Indian Ridge (17°–50°E), J. Geophys. Res. 97 (1992) 19771–19790.
[67] J.J. Mahoney, W.M. White, B.G.J. Upton, C.R. Neal, R.A. Scrutton, Beyond EM-1: lavas from Afanasy–Nikitin Rise and the Crozet Archipelago, Indian Ocean, Geology 24 (1996) 615–618.
[68] M. Rehkämper, A.W. Hofmann, Recycled ocean crust and sediment in Indian Ocean MORB, Earth Planet. Sci. Lett. 147 (1997) 91–106.
[69] C. Demets, R.G. Gordon, D.F. Argus, S. Stein, Current plate motions , Geophys. J. Int. 101 (1990) 425–478.
[70] C.H. Langmuir, R.D.J. Vocke, G.N. Hanson, S.R. Hart, A general mixing equation with applications to Icelandic basalts, Earth Planet. Sci. Lett. 37 (1978) 380–392.